On the Origin of Galactic Cosmic-Ray Electrons

G. E. Allen, R. Petre
NASA/Goddard Space Flight Center, LHEA, Code 660, Greenbelt, MD 20706

E. V. Gotthelf
Columbia Astrophysics Laboratory, Pupin Hall, Columbia University, 550 West 120th St, New York, NY 10027

J. W. Keohane
North Carolina School of Science and Mathematics, P. O. Box 2418, Durham, NC 27705

We present the RXTE PCA X-ray spectrum of SN 1006. This data exhibits evidence of high-energy non-thermal X-ray emission. An analysis of the RXTE PCA data and data from the ASCA SIS and ROSAT PSPC detectors suggests that the entire broad-band X-ray spectrum of SN 1006 may be fit with a single non-equilibrium ionization thermal component and a non- thermal component described by a broken power law with a low-energy photon spectral index of about 2.1 and a high-energy index of about 3.0. The shape of the non-thermal spectrum and a comparison of low- and high-energy X-ray images of SN 1006 with one another and with a radio image of the remnant suggest that the only plausible description of the non-thermal X-ray emission of SN 1006 is synchrotron radiation from 10-100 TeV electrons. The inferred properties of the cosmic rays in SN 1006 support the idea that Galactic cosmic rays are predominantly accelerated in supernova remnants.

I. INTRODUCTION

For many years the X-ray emission of shell-type (as opposed to plerionic) supernova remnants was modeled in terms of only the thermal emission of hot plasmas. However, it has recently become clear that at least some young shell-type supernova remnants (SN 1006 [1] [2], Cas A [3], G347.3−0.5 [4], IC 443 [5]) produce non-thermal emission as well. At least for SN 1006 and Cas A, the only plausible description of the non-thermal X-ray emission is synchrotron emission by 10–100 TeV electrons [2]. The non-thermal X-ray spectra of these two remnants are qualitatively consistent with simple models of the radio-to-X-ray synchrotron spectra, but are inconsistent with the predicted shapes and flux levels of other processes such as bremsstrahlung emission or inverse Compton scattering of the cosmic microwave background radiation. Furthermore, the high-energy (i.e. non-thermal–dominated) X-ray images differ substantially from lower-energy (thermal-dominated) X-ray images [6], but are similar to the radio synchrotron images of the remnants [7]. These two clues provide very-strong support for the idea that the non-thermal X-ray emission of SN 1006 and Cas A is synchrotron radiation. The presence of very-high–energy electrons in SN 1006 is corroborated by the detection of TeV gamma-ray emission from this remnant [8].

These results have very important implications for the study of Galactic cosmic-ray acceleration. Galactic cosmic rays, up to an energy of about 3000 TeV (the "knee"), are thought to be predominantly accelerated in the shocks of supernova remnants. Since the shock-acceleration process of supernova remnants depends on the magnetic rigidity of the particles, it may be the case that the cosmic-ray particles at 3000 TeV are principally iron and that protons (and electrons) are only accelerated to energies of about 100 TeV [9]. However, it has been difficult to confirm that supernova remnants accelerate particles to such high energies. Although previous radio and gamma-ray observations of remnants reveal evidence of non-thermal particles in many supernova remnants, these results are limited to particle energies ($\lesssim$ 10 GeV) that are well below 100 TeV (except for the TeV gamma-ray results of Tanimori *et al.* [8]. The non-thermal X-ray data of SN 1006 provided the first evidence that supernova remnants accelerate particles to very-high energies [1] [10]. We present an analysis of the entire broad-band X-ray spectrum of SN 1006, describe the thermal and non-thermal models fitted to the spectrum, and discuss the implications of the results for Galactic cosmic-ray acceleration.

II. DATA AND ANALYSIS

Between 1996 Feb 18 and 1996 Feb 20 SN 1006 was observed for 27 ks at a location on the north-eastern rim ($\alpha_{2000} = 15^{\rm h}4\overset{\rm m}{.}0$, $\delta_{2000} = -41°48'$) and for 26 ks on the south-western rim ($\alpha_{2000} = 15^{\rm h}1\overset{\rm m}{.}8$, $\delta_{2000} = -42°6'$) using the Proportional Counter Array (PCA) on the Rossi X-Ray Timing Explorer (RXTE) satellite. The PCA is a spectrophotometer comprised of an array of five co-aligned proportional counter units that are mechanically collimated to have a field-of-view of 1° FWHM [11]. The array is sensitive to photons that have energies between about 2 and 60 keV and has a maximum collecting area of about 7000 cm^2. The PCA data was screened to remove the time intervals for which (1) one or more of the five proportional counter units is off, (2) the detectors are pointed within 10° of the limb of the Earth, (3) the background model is not well defined, and (4) the nominal pointing direction is $> 0\overset{\circ}{.}02$ from the specified pointing direction in either right ascension or declination. After using these selection criteria, 7 ks of the data of the north-eastern and 11 ks of the data of the south-western pointings were used in the analysis.

The present analysis also includes 128 ks of data obtained with the Solid-state Imaging Spectrometers (SIS) on the Advanced Satellite for Cosmology and Astrophysics (ASCA) and 6 ks of data obtained with the Position-Sensitive Proportional Counter (PSPC) on the Röntgen satellite (ROSAT). Separate analyses of the data from these X-ray instruments has been published [1] [6].

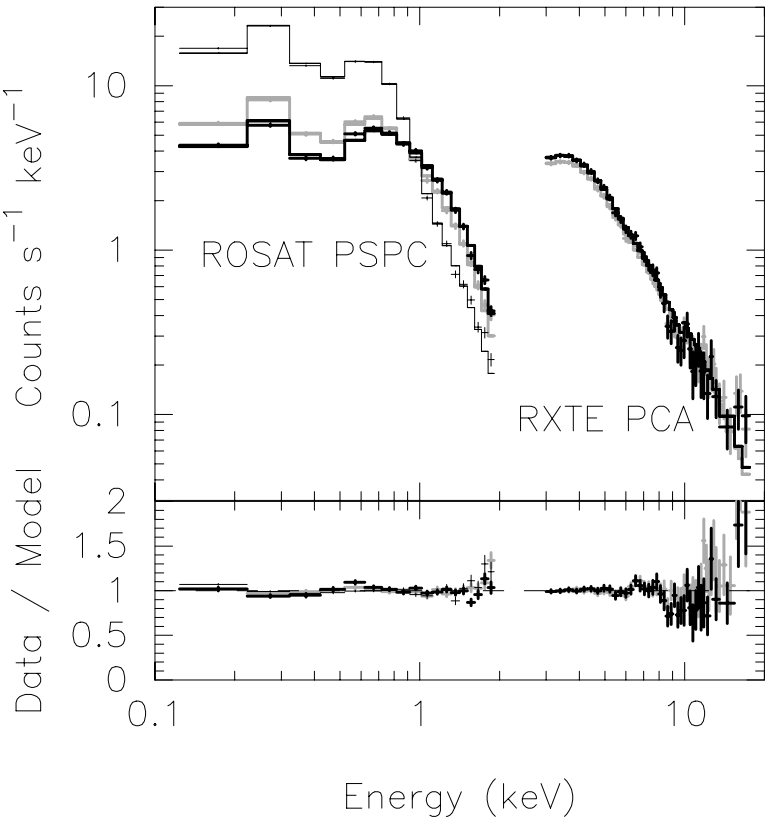

FIG. 1. A comparison of the RXTE PCA and ROSAT PSPC spectra of SN 1006 and the best fit spectral model. The top panel includes the data for the south-western rim (thick solid lines), north-eastern rim (thick stippled lines), and the center (thin solid lines) of the remnant. The histograms through the data are the results of the best-fit model. The lower panel depicts the ratios of the data to the model. The three spatial regions are mutually exclusive for the ROSAT data and include virtually all of the remnant. The same line styles are used for the PCA data to distinguish between the results obtained when the RXTE satellite was pointed at the south-western rim and when it was pointed at the north-eastern rim. However, the entire remnant is is the field-of-view of the PCA at both pointing positions.

The RXTE, ASCA, and ROSAT data were fit simultaneously using version 10.0 of the spectral-fitting software package XSPEC. Since Koyama *et al.* [1] report evidence of both thermal and non-thermal emission, the spectral fits were performed using several combinations of thermal and non-thermal emission models. The entire broad-band X-ray spectrum is fitted best ($\chi^2/\nu = 1109/729$) by a model that includes a broken power-law component and a non-equilibrium ionization component [2]. Table I lists the fitted parameters of this model.

A broken power law is not a physical model. We have used it to approximate a gradually steepening non-thermal spectrum as is expected [12] if the non-thermal X-ray emission is produced by synchrotron radiation. The shape and normalization of the broken power law component of the northeastern limb is consistent with the shape and normalization of the broken power law component of the south-western limb. As indicated by a comparison of the difference of the values of the low- and high-energy spectral indices of the broken power-law model, the non-thermal spectrum steepens with increasing energy (table I). The value of the break energy $E_{\rm b} = 1.85 \pm 0.20$ keV is not physically meaningful. This value is sensitive to the transition from the relatively low count-rate portion of the ROSAT PSPC spectrum to the relatively high count-rate portions of the ASCA SIS and RXTE PCA spectra.

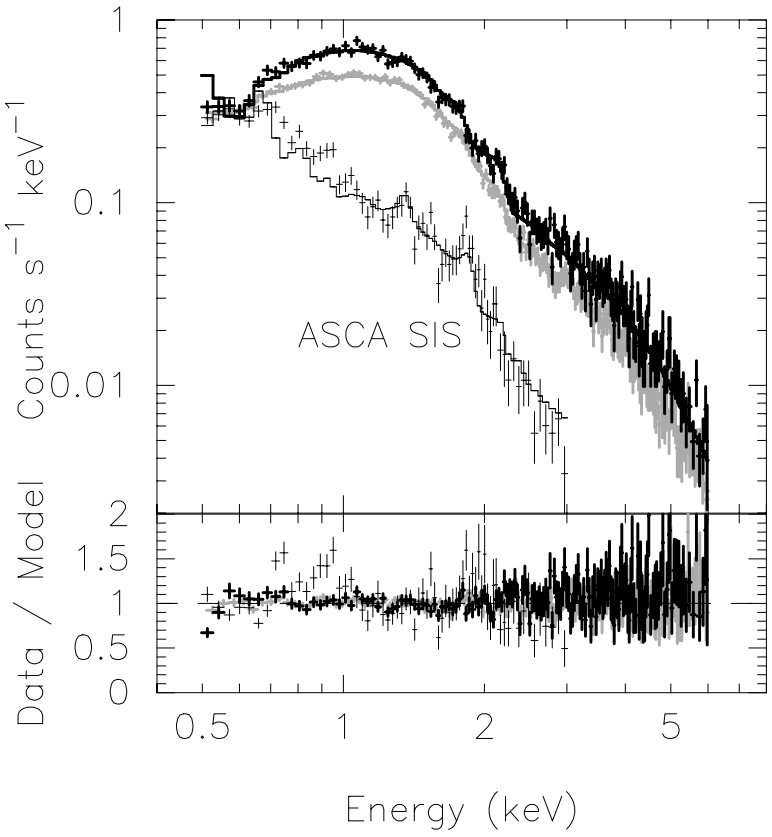

FIG. 2. A comparison of the ASCA SIS spectra of SN 1006 and the best fit spectral model. The contents are described in the caption of figure 1. The three spatial regions are mutually exclusive and include only a small portion of the entire remnant.

The best-fit thermal model is the non-equilibrium ionization model based on the work of Hamilton *et al.* [13]. The shape of the thermal continuum is specified by the shock temperature $T_{\rm s}$ and the quantity $n_0^2 E_0$, where n_0 is the ambient density of interstellar hydrogen and E_0 is the initial kinetic energy of the ejecta. The best-fit values of $T_{\rm s}$ and $n_0^2 E_0$ are determined by the thermal emission component of SN 1006. For example, within the statistical uncertainties, the same values for these two parameters are obtained if only the ASCA SIS spectrum of the central region of SN 1006 is used. The relative elemental abundances of the elements O, Ne, Mg, and Si have been included in the fit because the ASCA SIS spectrum of a central region of SN 1006 exhibits atomic–emission-line features associated with these elements [1]. The relative abundances of S and Ca have been fixed to be the same as the abundance of Si. This

situation is more or less consistent with a model of type Ia supernovae [14]. Since the fit is not significantly improved if the relative abundances He, C, N, Fe, or Ni are included in the fit, these five abundances have been set to be the same as the relative elemental abundances of the solar system [15]. The relative abundances of all but Si, S, and Ca are consistent with the solar abundances of the elements.

III. DISCUSSION

The X-ray emission of the north-eastern and south-western limbs of SN 1006 that is modeled using a broken power-law is almost certainly non-thermal. Previous attempts to describe this emission in terms of thermal models have been unsuccessful [16]. These models fail to describe both the spatial and spectral distribution of the emission. In addition, fits to the broad-band X-ray spectrum of SN 1006 suggest that at least three thermal plasmas with temperatures ranging from 0.6 keV to 7 keV are needed to describe the spectrum. Furthermore, the distribution of the hot thermal gas would have to be consistent with the observation that the central region of the remnant exhibits strong atomic emission line features while the north-eastern and south-western limbs have essentially featureless spectra. Since it is difficult to satisfy these requirements using realistic assumptions about the conditions of the thermal plasmas and the circumstellar material, it appears that the only plausible conclusion is that the X-ray emission of the limbs is non-thermal.

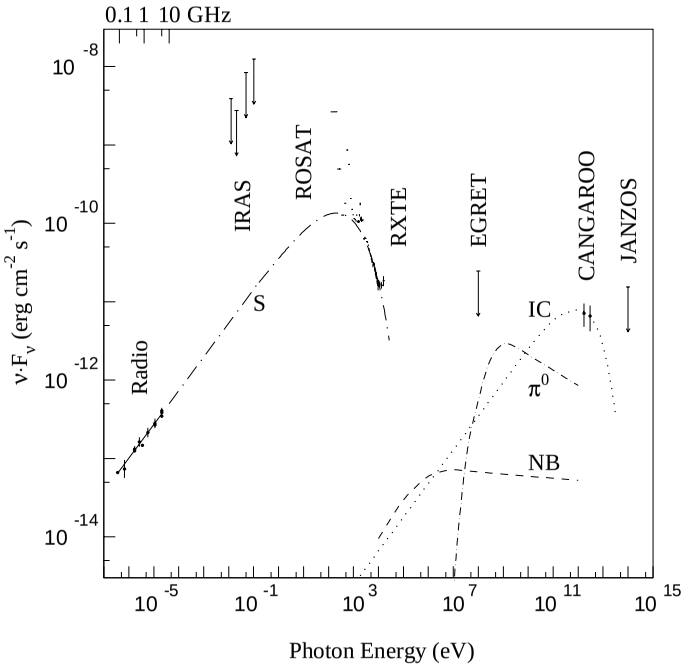

FIG. 3. The photon energy flux spectrum of SN 1006 from radio to gamma-ray energies. The data sets, which are labeled vertically, include several radio results [17], the IRAS infrared upper limits of Arendt [18], the ROSAT PSPC and RXTE PCA results of this paper, the EGRET gamma-ray upper limit of Hartman *et al.* [19], the gamma-ray results of the CANGAROO collaboration [8], and the gamma-ray upper limit of the JANZOS collaboration [20]. The four model spectra are estimates of the photon energy fluxes produced by synchrotron radiation (S), inverse Compton scattering on the cosmic microwave background radiation (IC), the decay of neutral pions (π^0), and bremsstrahlung emission of the non-thermal electrons (NB).

Of the possible non-thermal X-ray emission models, only synchrotron radiation is consistent with both the spatial and spectral distribution of the X rays. For example, the non-thermal spectrum is significantly better fit by a broken power law than a power law. Since a broken power law is not a physical model, it presumably describes a spectrum that

steepens with increasing energy. Such a spectrum is consistent with X-ray synchrotron radiation, but not non-thermal bremsstrahlung emission or inverse Compton scattering [10]. In addition, the broad-band radio-to-X-ray spectrum is qualitatively consistent with a simple model of the synchrotron spectrum of a remnant (fig. 3). Furthermore, the high-energy non-thermal–dominated X-ray image of SN 1006 [6] is similar to the radio synchrotron image of the remnant [7] and both are considerably different from the low-energy thermal-dominated X-ray image [6]. These spatial results suggest that the high-energy X-ray emission and radio emission are produced by a similar emission mechanism and that this mechanism differs from the thermal bremsstrahlung process producing the low-energy thermal X-ray flux. Collectively, these clues provide very strong evidence that the X-ray emission of the limbs of SN 1006 is dominated by synchrotron radiation from very–high-energy electrons.

Other possible emission processes fail to describe one or more of these clues. For example, the non-thermal emission is not consistent with bremsstrahlung radiation from non-thermal electrons because the X-ray spectra of the limbs are dominated by non-thermal emission. In this case, most of the electrons would have to be non-thermal as opposed to thermal, which is unrealistic. If the emission is non-thermal bremsstrahlung, the high-energy X-ray image should be similar to the low-energy X-ray image instead of the radio image. Furthermore, a simple model of the non-thermal bremsstrahlung spectrum of SN 1006 is inconsistent with both the shape and the flux level of the X-ray spectrum of the remnant (fig. 3). For these reasons, the non-thermal emission of SN 1006 is not produced by non-thermal bremsstrahlung radiation.

Similar arguments about the X-ray and radio images and about a model of the inverse Compton emission of SN 1006 (fig. 3) reveal that inverse Compton scattering of GeV electrons on the cosmic microwave background radiation is inconsistent with the non-thermal X-ray emission of SN 1006.

The only other potential X-ray emission mechanism is a pulsar. Willingale *et al.* [6] argue that the bright north-eastern and south-western limbs are produced by beams of relativistic electrons from a compact object. However, no evidence has been found at any wavelength to support the existence of pulsar jets, a point-like source near the center of the remnant, or pulsations. Furthermore, the remnant of a type Ia supernova, which SN 1006 is identified to be, is not expected to contain a compact object. Therefore the non-thermal X-ray emission of SN 1006 can only be described by synchrotron radiation.

The detection of X-ray synchrotron emission from SN 1006 has important implications for Galactic cosmic-ray acceleration. For example, since the X-ray synchrotron spectrum is much steeper than the radio synchrotron spectrum (fig. 3), the roll over in the synchrotron spectrum at about 100 eV is associated with an exponential cut off in the electron spectrum of the remnant. If we know what the magnetic field strength in the remnant is we can compute the corresponding e-folding energy of the exponential cut off. Since SN 1006 is observed to emit TeV inverse Compton gamma-ray emission [8], it is possible to use the TeV emission to determine the normalization of the electron spectrum. This normalization and the radio flux, which depends on the electron spectrum and the magnetic field strength, imply a magnetic field strength $B \sim 10$ μG. This estimate is sensitive to the shape of the electron spectrum and the relative effective volume filling factors of the cosmic-ray electrons and the magnetic field. Therefore, the estimated field strength should be regarded as an order-of-magnitude estimate. With $B \sim 10$ μG and a roll off in the synchrotron spectrum as shown in figure 3, the exponential e-folding energy of the electron spectrum is estimated to be about 20 TeV. This estimate is somewhat below 100 TeV. If this estimate is accurate, the results may indicate that the cosmic-ray electrons in SN 1006 have not yet reached their maximum energy, that SN 1006 does not accelerate cosmic-ray electrons to energies as high as 100 TeV, or that the maximum energy of the electrons (but not the nuclei) is regulated by radiative losses. In any event, SN 1006 is a significant source of Galactic cosmic-ray electrons.

Two other clues support the idea that SN 1006 is a significant source of Galactic cosmic rays. The first clue is that the radio spectral index of SN 1006 $\alpha = 0.57$, which corresponds to a differential spectral index of the GeV electrons , $= 2.14$ $(= 2\alpha + 1)$. This index is consistent with the index expected for cosmic-ray accelerators because the observed differential spectral index of the cosmic-ray protons observed at Earth (, $= 2.8$ [21]) less the inferred spectral steepening due to an energy-dependent escape of the cosmic rays from the Galaxy (Δ, $= 0.6$ [22]) is about 2.2.

The second clue also stems from an analysis of the radio spectral data. The radio data of a remnant may be used to estimate the total energy of the cosmic-ray particles in the remnant. This estimate depends on some assumptions about the strength of the magnetic field and about the cosmic-ray electron and proton spectra of the remnant. For simplicity, we assume (1) that the magnetic field of SN 1006 $B = 10$ μG, (2) that the cosmic-ray electron and proton spectra are described by $dN_{\rm e,p}/dE \propto (E + m_{\rm e,p}c^2)(E^2 + 2m_{\rm e,p}c^2E)^{-(\Gamma+1)/2}e^{-E/\epsilon}$ [23], (3) that the high-energy spectral indices (,) of the electrons and protons are the same, (4) that the e-folding energy of the exponential cut off energy $\epsilon = 20$ TeV, and (5) that non-thermal electrons outnumber non-thermal protons by a factor of 1.2. The last assumption follows from the assumptions that the relative elemental abundances of the cosmic rays are comparable to the relative elemental abundances of the solar system, that all hydrogen and helium nuclei are fully ionized, and that equal proportions of electrons and nuclei are non-thermal. This set of assumptions naturally leads to the result that cosmic-ray protons outnumber cosmic-ray electrons by a factor ~ 100 at 1 GeV, as is observed at Earth. Using these assumptions, we find that, at the present, the total energy of the cosmic-ray particles in SN 1006 $U_{\rm cr} \sim 2 \times 10^{49}$ erg. This order-of-magnitude estimate is comparable to estimates of the total energy that is needed, on average, per remnant, over their lifetimes ($\sim$ 3–10^{49} erg [24]).

IV. CONCLUSION

We present the RXTE PCA X-ray spectrum of SN 1006. This data exhibits evidence of high-energy non-thermal X-ray emission. An analysis of the RXTE PCA data and data from the ASCA SIS and ROSAT PSPC detectors suggests that the entire broad-band X-ray spectrum of SN 1006 may be fit with a single non-equilibrium ionization thermal component and a non- thermal component described by a broken power law with a low-energy photon spectral index of about 2.1 and a high-energy index of about 3.0.

This shape of the non-thermal spectrum and a comparison of low- and high-energy X-ray images of SN 1006 with one another and with a radio image of the remnant suggest that the only plausible description of the non-thermal X-ray emission of SN 1006 is synchrotron radiation from 10–100 TeV electrons. The detection of X-ray synchrotron radiation from SN 1006 has important implications for the acceleration of Galactic cosmic rays. A simple model of the radio-to-X-ray synchrotron spectrum implies that the exponential e-folding energy of the cut off in the electron spectrum of SN 1006 $\epsilon \sim 20$ TeV. This energy is only slightly below an anticipated cut-off energy $\epsilon = 100$ TeV. In addition, the radio spectral index implies that the differential spectral index of the electron spectrum at GeV energies (, $= 2.14$) is consistent with the spectral index inferred for the Galactic cosmic-ray accelerators (, $= 2.2$). Furthermore, an estimate of the total energy of the cosmic rays in SN 1006 $U_{\rm cr} \sim 2 \times 10^{49}$ erg (assuming that nuclei are also accelerated), which implies that SN 1006 accelerates as many cosmic rays as are needed, per supernova remnant, to explain the observed population of Galactic cosmic rays. Therefore the inferred properties of the cosmic rays in SN 1006 support the idea that Galactic cosmic rays are predominantly accelerated in supernova remnants.

---

[1] K. Koyama *et al.*, Nature. **378**, 255–58 (1995).;
[2] G. E. Allen *et al.*, In preparation. (1999).
[3] G. E. Allen *et al.*, Astrophys. J. Lett. **487**, L97–L100. (1997).
[4] K. Koyama *et al.*, Publ. Astron. Soc. Jpn. **49**, L7–L11. (1997); P. Slane *et al.*, Astrophys. J. Submitted. (1999).
[5] J. W. Keohane *et al.*, Astrophys. J. **484**, 350–59 (1997).
[6] R. Willingale *et al.*, Mon. Not. R. Astron. Soc. **278**, 749 (1996); S. S. Holt *et al.*, Publ. Astron. Soc. Pac. **46**, L151 (1994); J. Vink *et al.*, Astron. Astrophys. In press. (1999).
[7] S. P. Reynolds, and D. M. Gilmore, Astron. J. **92**, 1138 (1986); M. C. Anderson, and L. Rudnick, Astrophys. J. **441**, 307 (1995).
[8] T. Tanimori *et al.*, Astrophys. J. Lett. **497**, L25–28 (1998).
[9] P. O. Lagage, and C. J. Cesarsky, Astron. Astrophys. **125**, 249–57 (1983).

[10] S. Reynolds, Astrophys. J. Lett. **459**, L13–L16 (1996).
[11] K. Jahoda *et al.*, in EUV, X-ray and Gamma-ray Instrumentation for Space Astronomy VII, ed. O. H. W. Siegmund, and M. A. Grummin, Proc. SPIE, **2808**, 59 (1996).
[12] S. P. Reynolds, Astrophys. J. **493**, 375–96 (1998).
[13] J. S. Hamilton, C. L. Sarazin, and R. A. Chevalier, Astrophys. J. Suppl. Ser. **51**, 115 (1983).
[14] K. Nomoto, F.-K. Thielemann, and K. Yokoi, Astrophys. J. **286**, 644–658 (1984).
[15] E. Anders, and N. Grevesse, Geochimica et Cosmochimica Acta. **53**, 197 (1989).
[16] J. M. Laming, Astrophys. J. **499**, 309–314 (1998); A. J. S. Hamilton, C. L. Sarazin, and A. E. Szymkowiak, Astrophys. J. **300**, 698–712 (1986).
[17] M. R. Kundu, Astrophys. J. **162**, 17 (1970); D. K. Milne, Aust. J. Phys. **24**, 757 (1971); D. K. Milne, and J. R. Dickel, Aust. J. Phys. **28**, 209 (1975); F. R. Stephenson, D. H. Clark, and D. F. Crawford, Mon. Not. R. Astron. Soc. **180**, 567 (1977); R. S. Roger, Astrophys. J. **332**, 940 (1988)
[18] R. G. Arendt, Astrophys. J. Suppl. Ser. **70**, 181 (1989).
[19] R. C. Hartman *et al.*, Astrophys. J. Suppl. Ser. In press. (1999), figure 3.
[20] W. H. Allen *et al.*, Proc. 24th Int. Cosmic Ray Conf. (Rome). **2**, 447 (1995).
[21] K. Asakimori *et al.*, Astrophys. J. **502**, 278 (1998).
[22] S. P. Swordy *et al.*, Astrophys. J. **349** 625 (1990).
[23] A. R. Bell, Mon. Not. R. Astron. Soc. **182** 443 (1978).
[24] R. Blandford, and D. Eichler, Phys. Rep. **154** 1 (1987); R. E. Lingenfelter, In The Astronomy and Astrophysics Encyclopedia, ed. S. Maran, Van Nostrand Reinhold Publishers, 139 (1992).

TABLE I. Parameters of the Best-Fit Model.

Parameter	Value	90% Interval
Broken power-law component		
$n_{\rm H}$ [10^{20} atoms cm^{-2}]	5.60	5.04–6.24
$_{,\,1}$	2.08	1.94–2.20
$E_{\rm b}$ [kev]	1.85	1.66–2.05
$_{,\,2}$	3.02	2.86–3.19
K [10^{-3} photons cm^{-2} s^{-1} keV^{-1}]	6.20	5.86–6.54
Flux(0.1–2 keV) [10^{-10} erg cm^{-2} s^{-1}]	1.48	1.36–1.60
Non-equilibrium ionization component		
$T_{\rm s}$ [K]	10^8	$10^{7.25}$–10^8
$n_0^2 E_0$ [erg cm^{-6}]	10^{50}	10^{49}–10^{50}
He	1	...
C	1	...
N	1	...
O	1.6	0.81–8.9
Ne	0.31	0–3.1
Mg	2.0	0–9.8
Si	16	7.9–29
S	16	7.9–29
Ca	16	7.9–29
Fe	1	...
Ni	1	...
Flux(0.1–2 keV) [10^{-10} erg cm^{-2} s^{-1}]	2.63	2.34–3.03